

### Contents lists available at ScienceDirect

## Acta Astronautica

journal homepage: www.elsevier.com/locate/actaastro



## Research paper

# A flexible modular approach for the exploration and settlement of planetary environments



- <sup>a</sup> Department of Engineering and Architecture, University of Trieste, via A. Valerio 6/1, Trieste, 34127, Italy
- b Institute of Robotics and Mechatronics, German Aerospace Center (DLR), Münchener Str. 20, Wessling, 82234, Germany

### ARTICLE INFO

#### Keywords: Rover Space exploration Settlement Multi-body simulation Dynamics

#### ABSTRACT

Designing large precursor missions for planetary exploration and settlement is proving daunting due to several concurrent challenges: infrastructure needs to be modularized and standardized; modules need to be transported quickly, efficiently and reliably; using robots to assemble modular structures is a challenging problem; low terrain trafficability severely impair rover velocity and accessibility; use of in-situ resources (ISRU) is required to reduce launched mass; reliable power needs to be available during construction and operations. In this work, we propose an integrated framework for the exploration of planetary environments, the assembly of precursor bases and ultimately human settlement. The framework is centered on the TransRoPorter (TRP) robot in development at the DLR's Institute of Robotics and Mechatronics, and specially designed Payload Modules (PM) that make up the spine of the infrastructure. We show that most challenges can be tackled efficiently and effectively with our framework, by selecting a few use-cases: a crater-based water-ice extraction scenario and a sensor network assembly. We provide in-depth simulations that showcase the feasibility of the approach using the TRP-PM based solution.

## 1. Introduction

Since its inception, the exploration of space and in particular of planetary bodies, has been carried out mostly by single one-package probes [1]. With the notable exception of exploiting satellites as communication relays, e.g. CNSA's Tianwen-1 [2] or NASA/JPL's Mars Reconnaissance Orbiter [3], the focus has been, for the great part, about packing the scientific payload and the necessary sub-systems in the probe itself, thus making it as self-sufficient as possible [4].

In the light of recent planning about increasing the robotic and – further down the road – human presence on the Moon, Mars and asteroids, by the major space agencies [5,6], a new approach promises to be useful.

In particular, the focus is now on multi-agent exploration, using teams of diverse robotic systems to perform complex tasks autonomously [7–9]. The multi-expertise exploration strategies that are involved, require delivery systems which need to be flexible and modular, so as to allow for a diverse range of activities. An example is the construction of a moon base [10], where most of the infrastructure needs to be built prior to the arrival of astronauts: power plants, storage facilities, communication systems, repeaters, even In-Situ Resource

Utilization (ISRU) components, and habitats. Most of these would be required for an extensive robotic exploration strategy as well [8].

The Ingenuity helicopter and the Perseverance rover constitute the first example of cooperative robotized exploration [11]. Despite being originally a simple technology demonstrator, with a planned 30-sol operational life consisting of just five flights, the small helicopter went on for nearly three years, accumulating 72 flights and effectively assisting both navigational and planning tasks of Perseverance's operations team [12].

The design of currently operating rovers only allows for very low driving speed [7,13–15], mainly for reliability and to avoid shocks to the scientific payload. However, it is becoming increasingly clear that faster rovers are desirable when approaching multi-agent robotic exploration, infrastructure assembly and settlement in general [16–18]. This is due to the distance between the landing point and the infrastructure being generally non-negligible for three main reasons:

 Landing ellipses are large, and limit accurate touchdown of the spacecraft modules (e.g. MSL's ellipse was 7 by 20 km [19], Mars2020's was 6.6 by 7.7 km [20]),

E-mail addresses: sseriani@units.it (S. Seriani), matteo.caruso1993@gmail.com (M. Caruso), simone.cottiga@phd.units.it (S. Cottiga), pgallina@units.it (P. Gallina), martin.goerner@dir.de (M. Görner), armin.wedler@dir.de (A. Wedler).

https://doi.org/10.1016/j.actaastro.2025.09.083

Received 16 June 2025; Received in revised form 24 September 2025; Accepted 26 September 2025 Available online 4 October 2025

0094-5765/© 2025 The Authors. Published by Elsevier Ltd on behalf of IAA. This is an open access article under the CC BY license (http://creativecommons.org/licenses/by/4.0/).

<sup>\*</sup> Corresponding author.



Fig. 1. Artistic representation of the modular architecture framework on the surface of a planet. On the left, the carrier rover is shown; in the center, a high-gain antenna with a single solar panel array is visible, and on the right a multi-module solar array is shown in its deployed configuration.

- Landing in the vicinity of existing infrastructure is undesirable,
   i.e. possible damage due to unlikely but possible collision (direct),
   and due to plume-surface interaction [21] (indirect),
- Areas suitable for landing are not necessarily close to locations interesting for a base or a scientific investigation; a known conundrum since the Apollo landings, but still current [22].

However, faster rovers are challenging, due to inherently riskier operations (e.g. dynamic driving, high-speed collisions), requiring a higher degree of autonomy [23], and high performance rough terrain capabilities (e.g. suspension systems, shock and motion compensation) [16,17].

In the last decade especially, there has been considerable expansion of the field of articulated wheels rovers, i.e. mobility platforms where each wheel is mounted on a "leg" – essentially a robotic manipulator with 2 or more degrees of freedom, e.g. the sherpaTT rover [24], the TWAL rover [25] and others [26].

## 1.1. Vision and contributions

In this paper, in order to increase the potential for exploration, we propose an approach, illustrated in Fig. 1, which addresses the scalability of multi-agency and the issue of designing faster rovers, aspects that are generally not exploitable with the single-probe strategy; this is done through the following key objectives, which define our vision:

- Separating the locomotion apparatus (the carrier rover CR) from the payload itself (the payload module PM),
- Providing the rover with advanced rough terrain negotiation capabilities, i.e. an active suspension system, stance reconfigurability.
- Enabling the assembly of modular structures leveraging the rover manipulation capability,

The main feature of this approach is that the CR provides advanced transportation functions as well as precise positioning at the destination of the PMs. The system exploits a suitable docking connection [27] for grasping and connecting the module: the CR then acts as a mobile manipulator for the PM. The PMs can be designed to be assembled

to other modules, via the same docking adapter, which can provide several types of connections (e.g. mechanical, electrical, fluid).

In the following, we present the main contributions to the state-ofthe-art of this work.

- We propose our vision for a modular approach for robotic exploration and settlement support in planetary environments;
- We describe in detail a possible architecture for the approach, the core of which consists of a carrier rover and payload modules that implement the required functions; we give the perimeter of the activities and possible functions, along with a set of example applications;
- We describe a carrier rover in terms of functional requirements, structure and kinematics;
- We justify the approach by defining two specific scenarios, the installation of a sensor network and a water ice extraction procedure.
- We validate the approach by simulation, exploring the higherlevel parameter space of the rover kinematics configuration.

#### 1.2. Structure of the article

The paper is organized as follows: in Section 2, we outline our vision for exploration, and describe in detail the main aspects of the modular architecture centered on the TransRoPorter (TRP) carrier rover and payload modules; in Section 3 we present two use-case scenarios that justify the proposed architecture; in Section 4 we expand on the use-cases and validate them via a large numerical simulation campaign using the TRP as the main actor; finally, in Section 5, we summarize our findings and propose a wide range of possible avenues of research for the next future.

## 2. A modular architecture

In the context of a complex exploration endeavour, be it robotic or even precursory to human inhabitation, a great number of possibly mutually dependent activities should be carried out at the same time. The rover which is employed to allow the implementation of the modular architecture is designed to provide efficient loading capabilities for the modules; as mentioned, this is achieved by using both a docking interface and a manipulation system for the module. An illustration

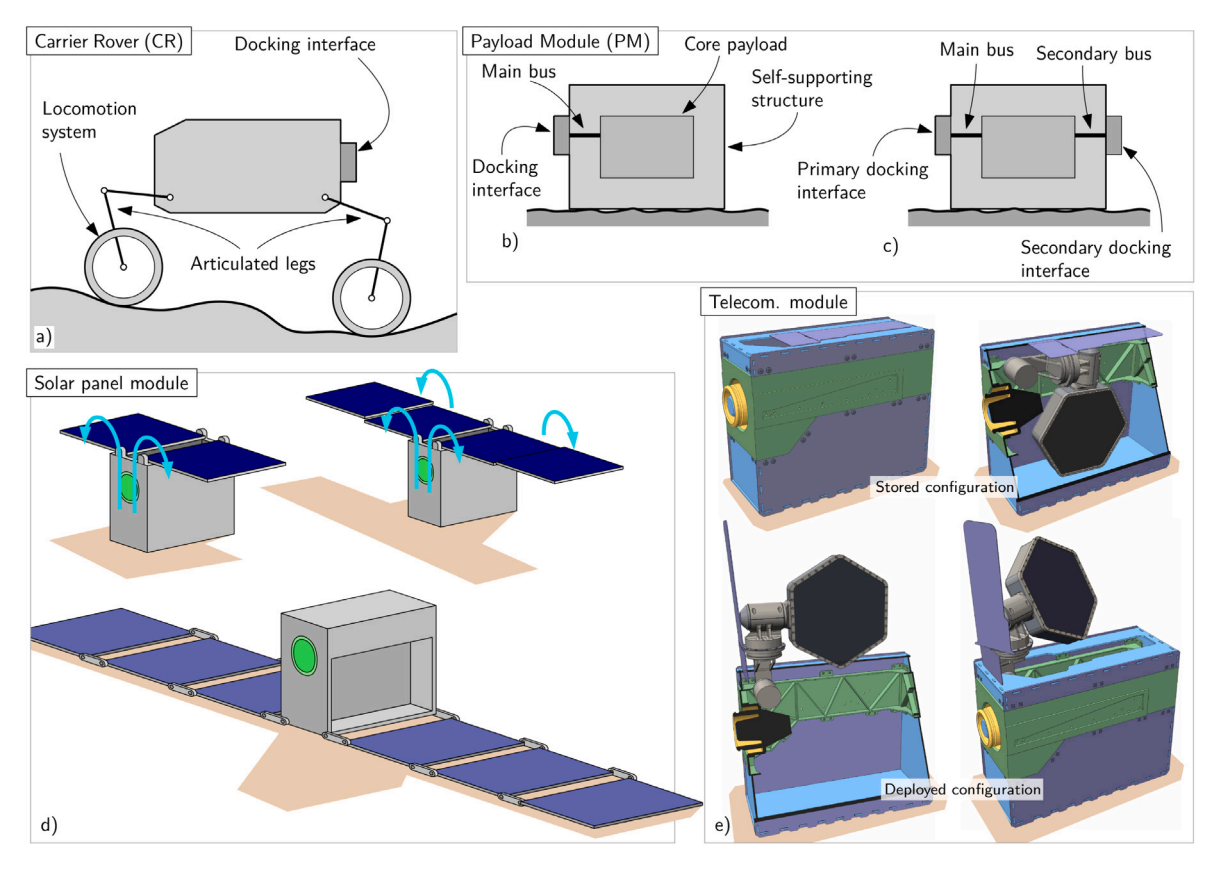


Fig. 2. High level system description. In (a) the rover is shown. In (b) the standalone module configuration is shown, equipped with one docking interface. In (c) the connected module configuration is shown, with the primary and secondary docking interfaces. In box (d) some possible configurations of a solar panel module are shown [28]. In box (e), the deployment of a high-gain directional antenna is shown as part of a conceptual communication-relay PM configuration.

of the main actors is shown in Fig. 1. The minimum configuration of the module can be defined as a system composed of a structural self-standing element, a docking adapter, and an active instrument, called core payload. The core payload is what defines the high-level primary function of the PM; basic low-level functions can be multiple. In Fig. 2, a diagram of the main components is shown. Based on the level of complexity and autonomy, the PM can be either active, or passive, where the latter cannot function by itself, i.e. without a docked active module or the rover.

#### 2.1. Motivations and merit

State-of-the-art planetary landing systems require flat and smooth terrain, whereas scientifically valuable sites are typically characterized by complex geological features [20]. At the same time, integrated exploration campaigns often necessitate establishing bases to support robotic and human activities. Building infrastructures directly at such sites therefore poses significant challenges if relying solely on in-place landing and assembly. In contrast, our approach decouples landing from infrastructure assembly, enabling base construction in geologically complex environments that offer the highest scientific return. More broadly, it supports the distributed deployment and assembly of assets across extensive terrains. To better frame the problem, we consider as an example the assembly of a hypothetical precursor base. Its infrastructure may consist of the following modules:

- Power generation module (x3), e.g. solar panels (see Fig. 2d,
- Power storage modules (x2), e.g. batteries,
- In-situ laboratory module (x1), akin to the CheMin instrument aboard the MSL rover [29],
- Manipulation module (x1), to manipulate modules and samples,
- Communication relay (x1), e.g. the module shown in Fig. 2e.

In this example, the scientifically relevant site is assumed to lie 20 km from the landing position. Neglecting module assembly operations, the total round-trip distance required for transport would be  $320\,\mathrm{km}$ . Given that current rovers are expected to achieve only about 200 m per day in autonomous mode  $(0.008\,\mathrm{km/h})$ , the assembly of the base would require an impractical 4.4 years, even under straight-line travel. These considerations highlight the need for rovers capable of repeated longrange traverses across rough terrain. At a modest pace of  $1\,\mathrm{km/h}$ , the operation time decreases to about two weeks (320 h), which reduces the duration to a feasible level.

## 2.2. Modules: classification and connectivity

Having described the concept of module, the most important general classification principle is its degree of autonomy. Based on this, two main kind of modules can be defined:

- Standalone modules. The PM can be designed as a self-sufficient system, containing the MCU (main computing unit), batteries and power generation system, communication system, and the active instrument. The self-sufficiency resides in the ability of the module to function without any direct physical connection to other modules or other systems, e.g. the rover. Nevertheless, two or more standalone modules can, in principle, cooperate using wireless communication. A diagram is shown in Fig. 2b.
- Non-standalone modules. When a PM is unable to perform its primary function without taking advantage of a direct physical connection to another specific system it is defined as nonstandalone: see Fig. 2c.

In order to enable complex architectures, each module should, in principle, be capable of connecting to others-whether to exchange information, distribute power, or allow manipulation. Furthermore, a degree of interaction with the carrier rover should also be supported, enabling handling. Such interactions can be facilitated through dedicated docking adapters [30]. The following outlines a set of connections particularly useful for planetary base-building and exploration activities.

- Mechanical connection: the fundamental structural interface that enables docking between modules, or between a module and the carrier rover.
- Electrical connection (data): provides the infrastructure for information exchange between modules.
- Electrical connection (power): enables power distribution to support onboard electronics and subsystems.
- Fluid connection: essential for many ISRU applications, such as propellant production.

In the following sections, an overview of the main tasks is given, which are possible either with the single modules or with specific combinations thereof.

#### 2.3. Prime activities

Complex endeavours like the construction, maintenance and upgrade of a planetary base, be it crewed or automated, require a vast amount of multidisciplinary systems and activities. This applies for the extensive exploration of celestial bodies as well. Power generation and storage, communication relay, life support management are only a few of the necessary tasks that need to be provided with good reliability and redundancy. Some of these prime activities are examined in the following,

- Power supply. Modularizing power management promises to considerably enhance the global operation efficiency of the system. Solar panel modules illustrated in Fig. 2d can be deployed on the surface and can provide a powered connection through the docking adapter. Modularization of power storage systems, e.g. batteries, allows expandable and redundant architectures.
- Communication relay. Long-range and high-bandwidth communication is a fundamental requirement for active planetary exploration devices. In self-contained systems (rovers, landers) a tradeoff is unavoidable, since weight and bulk are a major concern. However, exploiting a modular system based on a PM with a relay antenna, would unburden a notional rover of its long-range communication system. An example of this kind of module, equipped with a directional high-gain antenna, is shown in Fig. 2e.
- Fluid processing and storage. Liquids processing is chiefly important when manned systems are considered. Water, breathable atmosphere, waste fluids are the main actors in this application. By implementing a docking adapter that allows fluid transfer, a module can be conceived that serves as a processing or storage facility [27].
- In-situ instrumentation positioning. Extensive geological surveys often require the dissemination of sensor arrays on very large portions of the surface. Standalone modules equipped with the necessary sensors can be deployed by the carrier rover on arbitrarily large grounds.
- Carrier rover extension. The PM, as it is conceived in this work, can act as an extension of the carrier rover. Additional power storage, sensors, long-range communication are some possibilities. Especially interesting is the addition of a robotic arm.

In principle, these tasks can be executed either by standalone modules or by taking advantage of the composition of modules. However, based on the specific requirements, one approach could be more beneficial. For example, fluid storage benefits greatly of many non-standalone passive modules for the bulk of the storage, and few modules which take care of regulation or sensing; conversely, some in-situ instrumentation works best if self-contained, easing deployment procedures far from the base.

#### 2.4. High-level activities

The combination of prime activities allows for more complex ones to be executed. In this section, some of these high-level activities are examined. Based on the type of collaboration that the modules perform, the high-level activities can be classified as mono- or multi-disciplinary. Mono-disciplinary activities see the employment of a single kind of module, whereas the latter take advantage of at least two kinds of modules.

By exploiting the dual docking adapters illustrated in Fig. 2c multiple modules can be placed in series, provided that the ports are suitable to the task. In Fig. 1, an illustration of a multi-module solar array is shown; this type of architecture is composed of three modules of the type defined in Fig. 2d, which act as a charging base for the carrier rover – a *mono-disciplinary* task. In the same figure, the highgain antenna presented in Section 2.3 and in Fig. 2e is shown coupled to a power generating module; this is a type of *multi-disciplinary* task, in that it involves more than one kind of module.

#### 2.4.1. Assemblies

The first implementation where the benefits of a modular architecture are more apparent is that of infrastructure dedicated to complex tasks; these typically require large mass and volume footprints and are scarcely suitable for single-mission profiles.

- Precursor-base infrastructure. Future crewed bases typically require a precursor to be built robotically; as such, the framework could be taken advantage of by assembling communication relays (e.g. a battery module, solar panels, antenna, and transceiver/modem modules);
- In-situ experiments. Similarly, large-scale experiments can be modularized and implemented within this framework (e.g. laboratory modules similar to Curiosity's CheMin and SAM experiments [29], or NASA InSight's SEIS instrument [31]);
- ISRU and Large power plants. Implementing In-Situ Resources
   Utilization (ISRU) has been proved elusive because of demanding architectures and the requirement for many interconnected systems [32] (e.g. regolith and gas/fluid transfer, storing, and processing, interface to utilizers such as the base itself, rovers or crew-operated vehicles).

## 2.4.2. Networks

Several applications exist in planetary exploration where a network of standalone modules would be more efficient or even necessary. In the following some examples are given,

- Beacon network. Navigation on the surface of planetary bodies can be hard due to the non-trivial determination of the position of the rover with regards to the environment. Beacon networks can be used to triangulate the position, thus providing a surrogate for GNSS [33,34].
- Weather monitoring. Mars has seen increasing investigation in its weather and atmospheric system during the years. The deployment of a large scale, accurate permanent weather station network is useful for scientific, planning and safety reasons alike [35].
- Geophysical monitoring. Seismology is of paramount importance in the characterization of planetary bodies [36,37] and it would benefit from capillary sensor networks.

 Exploration of occluded locations. When line of sight with the communication equipment is not available because of occlusion, such as in the exploration of lava tubes or cave systems, repeaters should be provided in order to allow data relay [38].

Off-Earth robotic deployment of this type of networked infrastructure has yet to be done; its inherent complexity calls for methodologies which are flexible, robust and redundant.

#### 2.5. Carrier rover

The TRP Carrier Rover (CR) proposed in this framework is designed to be able to transport modules and manipulate the modules that constitute the complex architectures described in Section 2.4.

#### 2.5.1. Requirements

Since, e.g. in base-building, the assemblies outlined in Section 2.4.1 may have very different topologies, the rover-module architecture shall satisfy the following requirements:

- Manipulation and positioning of the module. This includes the loading/unloading operations and the assembly of the module to other already deployed modules;
- Transportation of modules across vast distances, i.e. measured in tens of kilometers;
- Interfacing with the modules, possibly to increase its own capabilities (e.g. an additional battery module);
- Rough terrain traversability. Planetary surfaces are generally characterized by obstacles of various size, sharp rocks and loose soil patches;
- Long-range and high-speed driving. Repeated drives over medium-long distances require a certain speed in order to keep driving times short.

The last point deserves to be analyzed in detail; it is well known that in state-of-the-art rovers [24], power is absorbed mainly by auxiliary systems such as heating elements, computers, communication equipment and the scientific payload (even when idle), rather than by the locomotion system itself. In principle, a rover which is not equipped with power generation should thus make the most of the energy stored in its batteries. Cutting down powered time of the auxiliary systems (especially the heaters needed for the electronics) by increasing the driving speed would bring a net energetic advantage, even considering larger power consumption in the locomotion system. Indeed, while the energy required to drive a certain distance is ideally independent of time, the energy absorbed by a heater (or an idle MCU) is dependent on time.

In order to perform the enabling tasks mentioned in the previous paragraph, as visible in Fig. 2a, the TRP exploits a hybrid locomotion system based on wheels with active steering, each mounted on a 2-d.o.f. manipulator, a concept investigated previously by Cordes et al. [24].

#### 2.5.2. Kinematics

It is worth noting that although three joints exist for each limb, only the first two (hip and knee) are equipped with an actuator. Furthermore, both are equipped with an elastic element in series to the actuator. The third joint (ankle) is rotationally fixed to the frame of the rover through a two-stage pulley system running inside the limb.

Since the hip and knee joints are actuated, there is an intrinsically increased reliability, redundancy, and the robot is more fault tolerant to single leg failure, this is because the robot can reconfigure itself and continue to drive with three legs. Additionally, given the assumption that the rover at any time stands upside down, then through appropriate control rules it can readjust its attitude to the operative one.

In this work we consider two possible alternatives for the kinematics of each leg: serial and parallel architectures.

- Serial architecture. The leg is a plain serial RRR kinematic chain starting from the hip-joint, the knee-joint and the ankle-joint. The actuator for the hip is placed between the thigh and the chassis of the rover, while the knee-actuator bridges the thigh with the shin. A simplified version which does not show the actuator is shown in Fig. 3b.
- Parallel architecture. The two actuators are both placed close to the hip-joint; note that, in particular, the knee-joint actuator is directly connected to the chassis of the rover; motion is transferred to the knee itself by a belt-drive. This type of kinematics can be found on some SCARA robots [39]. A simplified version without actuators is shown in Fig. 3c, while a comprehensive color-coded diagram of the internal structure and mechanisms of the limb is shown in Fig. 3g and h.

Contrary to the *serial* configuration, which operates as a simple RRR chain, in the case of the *parallel architecture*, the first link (thigh) is kept at an angle  $\vartheta_{i,1}$ , as visible in Fig. 3e in particular; the second link, which is rigidly connected to the pulley on the knee, can be made to rotate by an angle  $\varDelta\vartheta_{i,2}$ ; this is done by the knee actuator, located on the rover body, in the hip. Conversely, if we look at Fig. 3f, the knee actuator is kept still, while the hip actuator imposes a rotation  $\varDelta\vartheta_{i,1}$  to the 1st link; however, since the knee actuator is kept still, the 2nd link remains at the same orientation, albeit subjected to a translation given by the motion of the knee joint. The same is applied to the ankle joint, where a two-stage belt-drive is used to keep the foot level with the body.

### 2.5.3. Kinematics: serial vs. parallel

The parallel kinematics architecture decouples the rotation of the links, and thus greatly diminishes the torque required by the hip actuator compared to the *serial* case; indeed, being the knee actuator fixed to the frame, and not (as in the case of the *serial* architecture) on the previous link, the torque that is produced on the knee actuator itself by external forces (e.g. the weight of the rover, or an impact on the wheel) is not carried through to the hip-joint, but is directly supported by the rover's chassis. As expected, the *force* itself carries through the knee joint and to the hip-joint, but it can be received by appropriate bearings. Regardless of the elasticity/actuation scheme, the geometry of the limb is that of a 2-link serial planar manipulator. As such, the Denavit–Hartenberg parameters for the legs of the carrier rover are listed in Table 1, where the angles  $\vartheta_{i,j}$ , with j=1,2,3, are defined in Fig. 3h.

## 2.5.4. "XOAM" stances

Given that the legs' joints have almost complete freedom of motion (see Fig. 4b), a full evaluation of the infinite number of configurations would be intractable for the scope of this work. As such, we have carefully chosen four general *stances*, that well represent the main "seeds" of legs configurations. After all, the TRP rover has active legs, so in principle it is able to shift from one configuration to another with ease, although this aspect is out-of-scope at present. The configurations are referred to in the following as "XOAM", and are illustrated in Fig. 4a; each is associated to the uppercase letter the geometry resembles the most.

## 3. Approach justification

In order to provide validation to the approach presented in the previous sections, two scenarios are illustrated: the deployment of a sensor network and a base-building and support effort. In the former, traditional architectures are presented and compared to the proposed approach; efficiency in terms of payload versus required mass at atmospheric entry is then analyzed. Planetary bodies that lack an atmosphere are not considered explicitly in this work, however, similar considerations may apply.

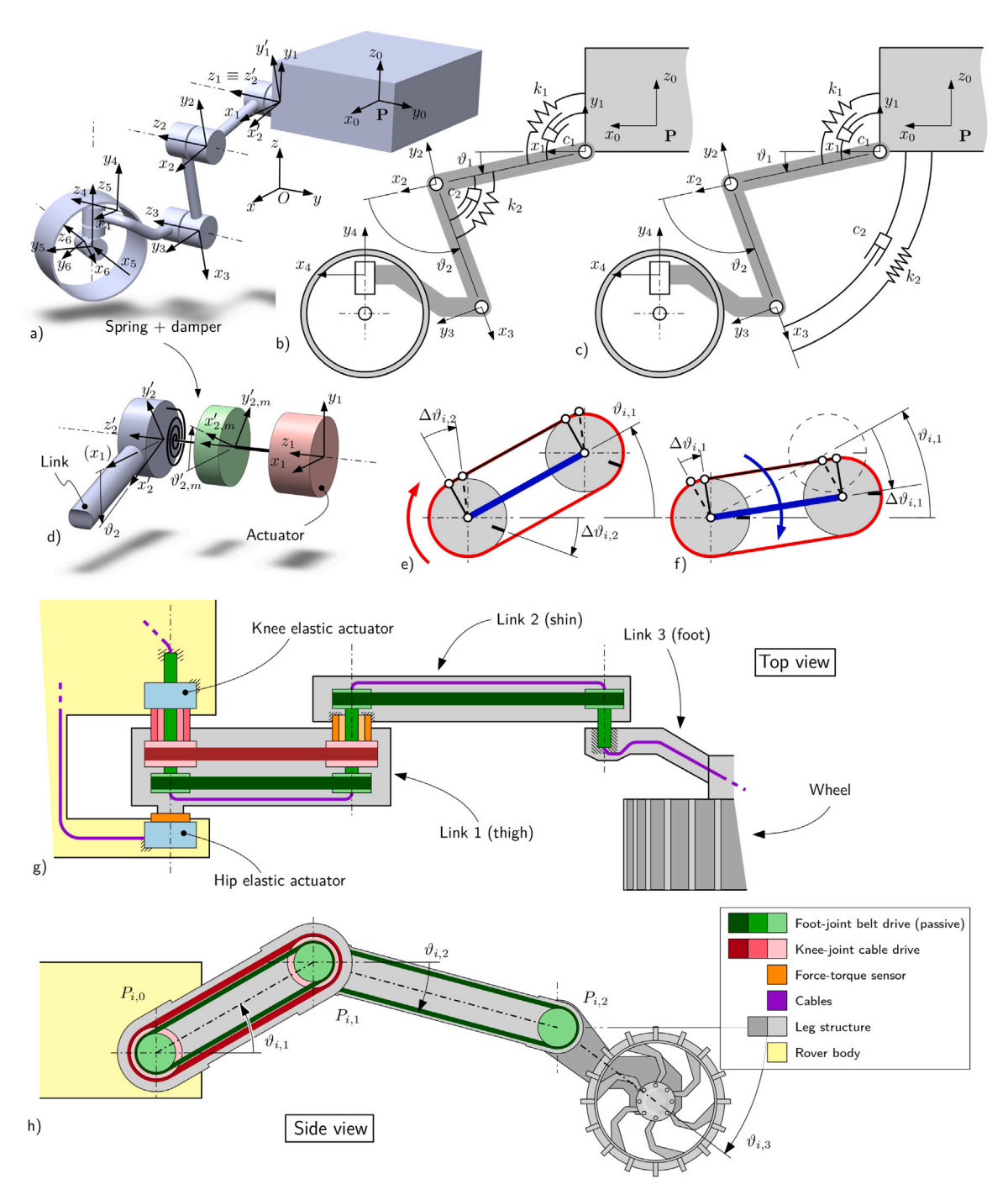


Fig. 3. Carrier rover diagram. In (a) the kinematics chain of a single leg is shown, along with the main frames of reference. In (b) and (c) the kinematics chain shows the location of the spring and dampers in the *serial* and *parallel* cases respectively. In (d) a complete diagram of a single actuated joint shows the actuator, the spring–damper system and the intermediate reference frames. In (e) the first link along with the knee belt system is shown when the hip joint is kept still at an angle, and the knee joint is made to rotate. In (f) the knee joint is kept still with respect to the frame and the hip joint is rotating. In (g) and (h) top and side views of the parallel-kinematics configuration implementation highlight the structure, and the location of the main components, such as drives, transmission, force–torque sensors, and the cable pass-through.

In the latter, which concerns base-operations, we make use of the capability of the rover to transport modules, to implement an ISRU scenario. The two scenarios are designed to offer elements to justify the proposed architecture when complex activities are planned; the sensor network scenario offers quantitative insight into the *effectiveness* and *efficiency* of the deployment logistics of the architecture, whereas the base-operations scenario shows – qualitatively and quantitatively

– that many of the characteristics of the proposed architecture can be leveraged to *enable* the planning of complex scenarios.

### 3.1. Scenario: Sensor network

Several areas of planetary research call for, or require, the use of extensive and distributed measurements on the ground. These include

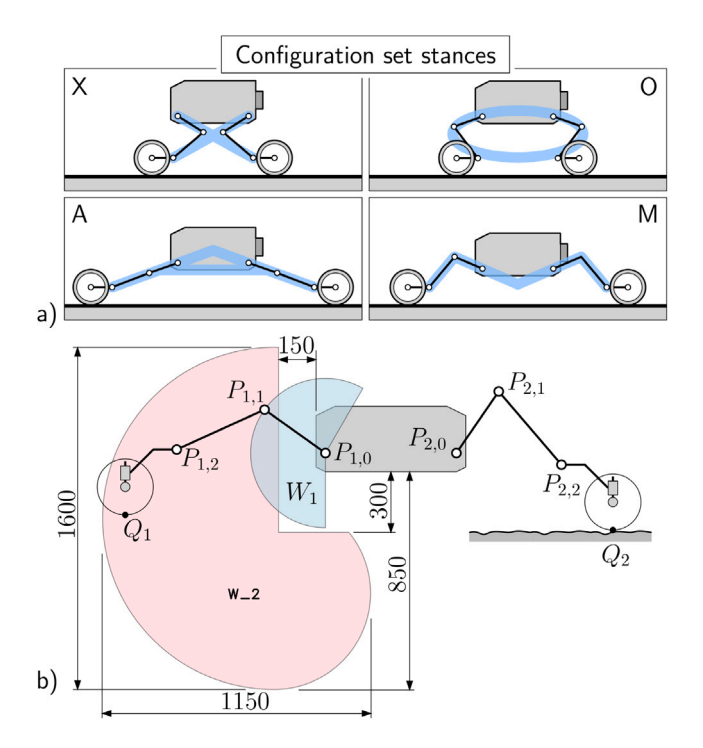


**Fig. 4.** Legs mobility of the TRP rover. (a) The four main stances, named X, O, A and M; (b) Reachability workspace for a single leg: the blue area shows the span of the first link, whereas the red area shows the reachability workspace of the contact point  $Q_1$  between the wheel and the ground.

Table 1
Denavit-Hartenberg parameters of the legs of the carrier rover. In the table's top section the D-H parameter table is shown for a general leg; in the bottom section, the values of the angles are shown for each stance.

Link	$a_j[m]$	$lpha_j$	$d_{j}$	$\phi_j$
Thigh	0.40	0	0	$\vartheta_{i,1}$
Shin	0.45	0	0	$-\theta_{i,1}-\theta_{i,2}$
Foot	0.20	0	0	$\begin{aligned} &-\vartheta_{i,1}-\vartheta_{i,2}\\ &\vartheta_{i,2}-\vartheta_{i,3} \end{aligned}$
Stance	$\vartheta_{i,1} [^{\circ}]$	$\vartheta_{i,2} [^{\circ}]$	$\theta_{i,3}[^{\circ}]$	
X	-160	20	0	_
0	-20	160	0	
A	-20	20	0	
M	20	60	0	

for example meteorology and seismology. In particular, seismic tomography is enabled by using a network of sensors on the surface [8]. However, the automated deployment of distributed infrastructure on planetary bodies has yet to be done. Three possible strategies are listed:

- Separate landers. Landers are targeted at various locations to form the required network.
- Autonomous mobile sensorized rovers. Originating from one or more landers, these rovers can traverse autonomously rough terrain to reach the required location and deploy the sensor.
- Carrier rover and payload modules. The payload modules containing the sensors are placed on target by the dedicated carrier rover. Both the modules and the rover are initially stored in the lander.

In Table 2 a qualitative analysis on the main advantages and draw-backs of the three strategies is presented. The first option involves using separate landers to target different locations; however, landing precision is low, e.g. the landing ellipse of NASA's Insight lander is 150 km long and 30 km wide [31]. This limits its applicability only when very sparse networks are considered. The other two options are

rover-based; they are able to achieve very high precision positioning at the expense of increased complexity. Of these, the strategy we propose, consisting of a carrier rover and payload modules, promises to be the most efficient in terms of total descent payload mass, provided that the number of deployed modules is substantial.

In order to quantitatively evaluate the three systems, a mass computation is provided in the following. Let us consider a sensor network composed of n sensor packages, each of mass  $m_{\rm PM}$ . In this scenario, Mars is the target planetary body on which the network is to be deployed. Recent existing missions on this planet are considered, in order to deliver an estimate of the mass budget and payload ratio for each possible approach, A, B or C. Thus, in Table 3 a detailed analysis of mass and mass ratios is illustrated for several surface missions on the Red Planet. The entry stage mass is an useful indicator of launch costs for a mission to Mars; from an energetic point of view, it includes launch from Earth, the Trans-Martian Injection burns, the possible aerobraking maneuvers at destination and finally the deorbit burn.

The TRP rover, described in Section 2.5, is atypical when compared against traditional rovers like MSL and MERs, in that it includes a PM docking system and has intrinsic manipulation capabilities. The hardware and support structures that allow for this are to be taken into account when computing projected mass values for a flight-ready system. Based on the added complexity of the actuation and structural requirements laid down in the relevant section of this paper, we consider a pejorative coefficient of  $\lambda_{\text{TRP}}$  when comparing the TRP's mass with that of a traditional rover. If we call  $\rho_{1,\text{L,avg}}$  the average value of  $\rho_1$  for the landers shown in Table 3, we can compute the projected total entry-stage mass of a mission consisting of n separate landers (strategy A), as follows,

$$m_{\text{entry,A}} = n_{\text{PM}} m_{\text{PM}} \rho_{1,\text{L,avg}}^{-1}. \tag{1}$$

Note that in this case, to simplify the mission architecture, we assume that there are  $n_{\rm PM}$  separate entry-stages, meaning that a deorbit burns is made for each lander, resulting in a more deterministic landing pattern. This also allows for multi-mission incremental approaches. Concerning approach B, where sensorized rovers are employed,

$$m_{\rm entry,B} = m_{\rm L} \rho_{2,\rm R,avg}^{-1} = \left( n_{\rm PM} m_{\rm PM} \rho_{3,\rm R,avg}^{-1} \right) \rho_{2,\rm R,avg}^{-1},$$
 (2)

where,  $\rho_{2,\mathrm{R,avg}}$  and  $\rho_{3,\mathrm{R,avg}}$  are the average values of the ratios  $\rho_2$  and  $\rho_3$  for rovers shown in Table 3. Finally, in approach C, where a single rover is used as a carrier for the  $n_{\mathrm{PM}}$  payload modules, the entry mass can be computed as follows,

$$m_{\text{entry},C} = m_{\text{L}} \, \rho_{2,\text{avg}}^{-1} \tag{3}$$

$$= \left( m_{\rm R} + n_{\rm PM} \, m_{\rm PM} \rho_{3,\rm avg}^{-1} \right) \, \rho_{2,\rm avg}^{-1} \tag{4}$$

$$= \left(\lambda_{TRP} m_{\text{PM}} \rho_{3,\text{R,avg}}^{-1} + n_{\text{PM}} m_{\text{PM}} \rho_{3,\text{L,avg}}^{-1}\right) \rho_{2,\text{avg}}^{-1}$$
 (5)

$$= \left(\lambda_{TRP} \rho_{3,R,avg}^{-1} + n_{PM} \rho_{3,L,avg}^{-1}\right) m_{PM} \rho_{2,avg}^{-1}, \tag{6}$$

where,  $m_{\rm R} = \lambda_{TRP} m_{\rm PM} \rho_{\rm 3,R,avg}^{-1}$  and  $\rho_{\rm 2,avg}$  is the average value of  $\rho_{\rm 2}$  for all platforms, both landers and rovers, since this case consists of both a fixed base containing the modules and a rover.

Assuming a payload mass of  $m_{\rm PM}=20\,{\rm kg}$ , Eq.s (1), (2) and (6) can be used to compute a *rough* estimate of the mass of the entry stage of a typical mission. Fig. 5 shows this value – along with the  $1\sigma$  confidence interval – as a function of the number of modules, for each approach, and for a few different values of the pejorative coefficient  $\lambda_{TRP}$ .

It is evident that, as expected, the separate lander option (A) is the least expensive in terms of entry-stage mass with respect to the other approaches. It is interesting to note that, while the sensorized rovers configuration promises to be cost-effective for  $n_{\rm PM} \leq 4$ , for larger architectures, i.e. comprising more components, a modular approach clearly shows dominance. Note that the scenario depicted in this section is conservative, in that it neglects scale factors that would take effect especially for the modular architecture. In particular, the coefficient  $\lambda_{\rm TRP}$  is likely to be non-linear and decreasing with  $n_{\rm PM}$ .

**Table 2**Qualitative comparison between deployment strategies for a sensor network.

Strategy	Advantages	Disadvantages
(A) Separate landers	<ul><li>Current technology (TRL 9)</li><li>High fidelity: no locomotion is necessary</li></ul>	<ul> <li>Imprecise positioning</li> <li>Relocation and reconfiguration are impossible</li> <li>High total mass</li> </ul>
(B) Mobile sensorized rovers	<ul> <li>Current technology (TRL 9)</li> <li>Possible relocation or reconfiguration</li> <li>Precise positioning</li> </ul>	<ul><li>High total mass</li><li>Complex operations due to multiple rovers</li></ul>
(C) Proposed carrier rover and payload module	<ul> <li>Possible relocation and configuration</li> <li>Precise positioning</li> <li>Low total mass</li> <li>Simple operations due to the single rover design</li> </ul>	<ul> <li>Needs development (Similar approaches: TRL</li> <li>4-6 [8,27])</li> <li>Complex interactions are required between robotic systems</li> </ul>

**Table 3**Analysis of mass budgets and computation of the related mass ratios for the most recent surface missions on Mars. Source NASA [40,41], CNSA [13].  $\rho_{i,avg}$  is the average value of  $\rho_i$  for the missions listed in the table.  $\rho_{i,R,avg}$  only considers the missions with a rover,  $\rho_{i,L,avg}$  only considers the landers missions. The Mars Pathfinder data are neglected in  $\rho_{i,avg}$  and  $\rho_{i,R,avg}$ .

\* inferred from 5000 (total mass) - 3715 (orbiter mass).

	$ ho_{i,L,avg}$	$ ho_{i,R,avg}$	$ ho_{i,avg}$	MSL	MER A/B	Mars Pathfinder	Zhurong	Perseverance	Phoenix	Beagle 2	Viking Lander I/II	Insight
Scientific payloadmass [kg]				75	8.74	7.98	25.9	59	59	9	91	50
Rover mass [kg]				899	173	11	240	1025	-	-	-	-
Landed mass [kg]				899	539	370	n.a.	1025	364	33.2	612	358
Entry stage mass [kg]				3300	836	585	1285*	3110	603	69	980	547
$m_{rov}/m_{entry}$ [%]	_	24.89	_	27.24	20.69	1.88	18.68	32.96	_	_	_	-
$\rho_2 = m_{landed} / m_{entry} [\%]$	_	41.56	51.58	27.24	64.47	63.25	n.a.	32.96	60.36	48.12	62.45	65.45
$\rho_4 = m_{payload}/m_{rov} [\%]$	_	7.49	_	8.34	5.06	72.55	10.79	5.76	_	_	_	-
$\rho_3 = m_{payload}/m_{landed} [\%]$	18.04	5.24	12.55	8.34	1.62	2.16	n.a.	5.76	16.21	27.11	14.87	13.97
$\rho_1 = m_{payload} / m_{entry} $ [%]	10.31	1.81	-	2.27	1.05	1.36	2.02	1.90	9.78	13.04	9.29	9.14
$m_{rov}/m_{landed}$ [%]	-	-	-	74.92	32.10	2.97	n.a.	100	-	-	-	-

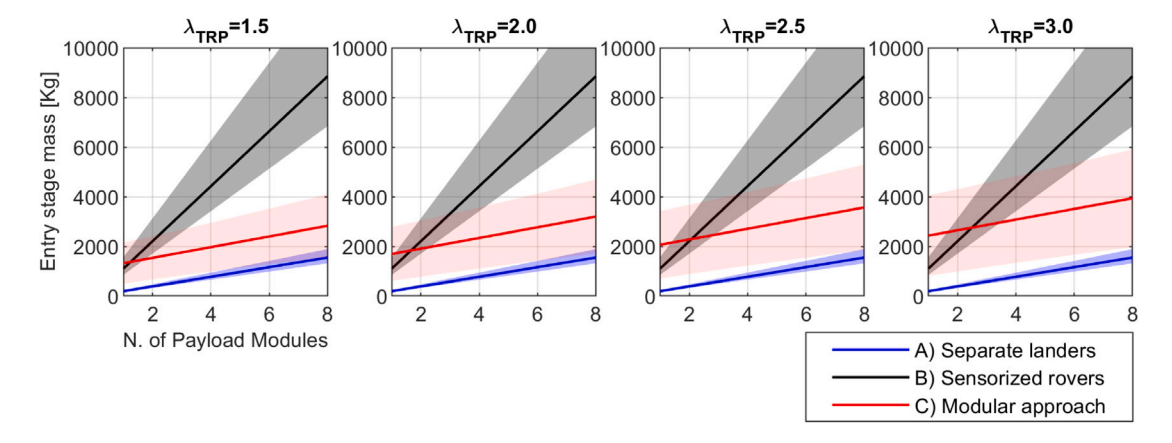


Fig. 5. Entry mass for the three approaches A, B and C, in relation to the number of modules. Note that approach C varies depending on the effective value of  $\lambda_{TRP}$ .

## 3.2. Scenario: Base operations - water ice extraction

In the context of In-Situ Resources Utilization (ISRU), much emphasis has been given to the widespread presence of water-ice close to the surface of Mars [42]. A similar situation is found on the Moon, where evidence of water-ice deposits have been found in the permanently shadowed regions of some craters [43]. Water ice is of obvious interest for exploration and settlement due to its use in producing Oxygen and water for life-support systems, rocket propellant, as support for agriculture and as radiation shielding [44,45].

We define a scenario that consists of a very general operation of water-ice extraction. Alternately, this can be considered interchangeable to a mining operation, or a sequence of sampling tasks. In order to represent the challenges faced when negotiating rugged terrain typical of craters, ridges and similar geological feature, we chose to consider a small-sized crater as the environment. The entire operation can be divided into three main phases: (A) prospecting, (B) installation of the infrastructure, (C) extraction and material transportation phase. The entire operation can be broken down in the following high-level sequence of events:

- A. **Prospecting:** evaluating the distribution of natural resources in the target environment;
  - Sample-collection module loading: the TRP loads the module from the base;

- Prospecting: the rover travels to the crater's basin and samples the terrain by positioning the module in the planned location;
- Transport: the rover carries the sample to the base; (Repeats until prospecting is complete...)
- Sample-collection module unloading: the rover unloads the module at the base;
- B. **Infrastructure installation**: preparation of the robotized extraction equipment at the site determined by prospecting;
  - Module loading: the TRP loads the relevant module following the base assembly plan;
  - Module transport: the rover transports the module to the extraction location:
  - Module positioning/assembly: the rover positions and possibly supports the assembly/connection of the module to previously installed modules;
    - (Repeats until installation is complete...)
- C. Extraction phase: supporting the extraction of the resource, by providing transport and manipulation;
  - Empty container module loading: an empty container module is loaded up by the TRP at the base;
  - Downhill travel: the TRP rover travels downwards towards the bottom of the crater, towards the location of previously deployed water-ice extraction infrastructure;
  - Full container module loading: another module container is loaded on the TRP;
  - Uphill transport: the TRP transports the full container module towards the base.
  - Full container module unloading: the TRP deposits the module in the unloading area.

(Repeats indefinitely...)

All activities called into play in this task breakdown can take great advantage of the capabilities of the proposed TRP modular architecture: mobility for sensor packages (prospecting), transport, manipulation and assembly of infrastructure (base-building), transport of raw material (base-operations, extraction).

## 4. Validation

In order to provide the baseline for a relevant and consistent analysis, in this section we provide a set of simulated use-cases that encompass a subset of the tasks laid out in Section 3. First, we give clear definitions regarding the simulation environment, its setup, and then we produce a description of the scenarios and an overview of results for each.

## 4.1. Simulation environment

The dynamic simulator adopted for the tests is Gazebo Classic [46]. The parameters of the simulated carrier rover are listed in Table 4. In order to simulate a realistic rover behavior whilst traversing soft soil, we developed a Gazebo plugin based on a custom version of the classic Bekker's terramechanic model [47,48], which computes and applies the interaction forces to each wheel as follows:

$$F = f(p_{soil}, p_{wheel}, p_{state}), (7)$$

where F is the vector of generalized forces/moments applied to a wheel,  $p_{soil}$  are the soil parameters, listed in Table 5,  $p_{wheel}$  are the wheel parameters, namely wheel radius, width, grousers height and grousers area ratio, and  $p_{state}$  are the wheel state parameters, namely commanded velocity, real velocity and load on the wheel. We devise two simulated scenarios, as such:

Table 4
Main parameters of the simulated carrier rover: mass and dimension of the links, stiffness and damping coefficients of the two active joints (see Fig. 3b and c for their locations in the *serial* and *parallel* cases).

Entity	Mass [kg]	Size*[m]	Stiffness [N m/rad]	Damping [N m s/rad]
Chassis	66.8	$0.9 \times 0.7 \times 0.3$		
Thigh	2.8	$0.05 \times 0.40$		
Shin	2.0	$0.05 \times 0.45$		
Foot	2.6	$0.05 \times 0.20$		
Wheel	1.7	$0.15 \times 0.15$		
Hip			500	50
Knee			500	50

 $<sup>^*</sup>$  chassis (box): size = length x width x height; other links (cylinders): size = radius x length.

**Table 5** Parameters of the terrains implemented in the simulations, where  $k_c$ ,  $k_{\phi}$  and k are the cohesive, frictional, and sinkage moduli, c is cohesion,  $\phi$  the friction angle, K the shear modulus, and n the sinkage exponent.

Parameter	Soil Direct #90 sand [47]	Mars simulant [48]	Dry sand [49]
$k_c [N/m^{n+1}]$	_	13.6×10 <sup>3</sup>	$0.99 \times 10^{3}$
$k_{\phi}$ [N/m <sup>n+2</sup> ]	_	$2259.1 \times 10^3$	$1528.43 \times 10^3$
$k[N/m^{n+2}]$	8×10 <sup>6</sup>	*	*
c [Pa]	$1\times10^{3}$	462.3	$1.04 \times 10^{3}$
$\phi$ [°]	29	35	28
K [m]	0.021	0.015	0.01
n [-]	**	**	**
$n_0 [-]$	1.46	0.92	1.10
$n_1$ [-]	0.01	0.5	0
n <sub>2</sub> [-]	0.74	0.5	0

<sup>\*</sup>  $k = k_c/b + k_\phi$ , with wheel width b [m].

- Material transport scenario. Fig. 6c, e and f show the small-sized crater environment for the *material transport* scenario, consisting in a 71×71 m mesh of 9800 triangular polygons and maximum altitude of 7.13 m. The mesh is divided in three layers, identified by the three colors in the figure, each one characterized by a different type of terrain.
- Long-range driving scenario. Meant to represent long-range driving during base-building or the deployment of sensors in large areas, it is shown in Fig. 6d, with a 1000×20 m mesh of about 38000 polygons and maximum altitude of 14.11 m. Similarly to the former, it is divided into three sections with different terrain material along the longest dimension.

For both scenarios the surface mesh has been generated based on Digital Elevation Maps of Mars in the Gale crater region, as shown in Fig. 6; the gravity acceleration applied to the simulated environment is  $g = 3.73 \,\mathrm{m\,s^{-2}}$ , consistent with that of Mars.

The characteristics of the three types of terrain are listed in Table 5. The soil distribution in the Crater environment is shown in the figure with the following order and colors: red) "Soil Direct #90 sand", green) "Dry sand", and orange) "Mars simulant"; for the long-range map, the soil is divided into three equally long sections with the same order.

#### 4.2. Control

In order for the carrier rover to follow the predefined paths, which will be discussed later, a simple path following controller was implemented. This relies on PID controllers to determine the high level linear and angular velocities commanded to the rover, according to its current position and heading with respect to the target path waypoint.

<sup>\*\*</sup>  $\begin{cases} n = n_0 + n_1 s, s \ge 0, \text{ with slip ratio } s \ [-]. \\ n = n_0 - n_0 s, s < 0 \end{cases}$ 

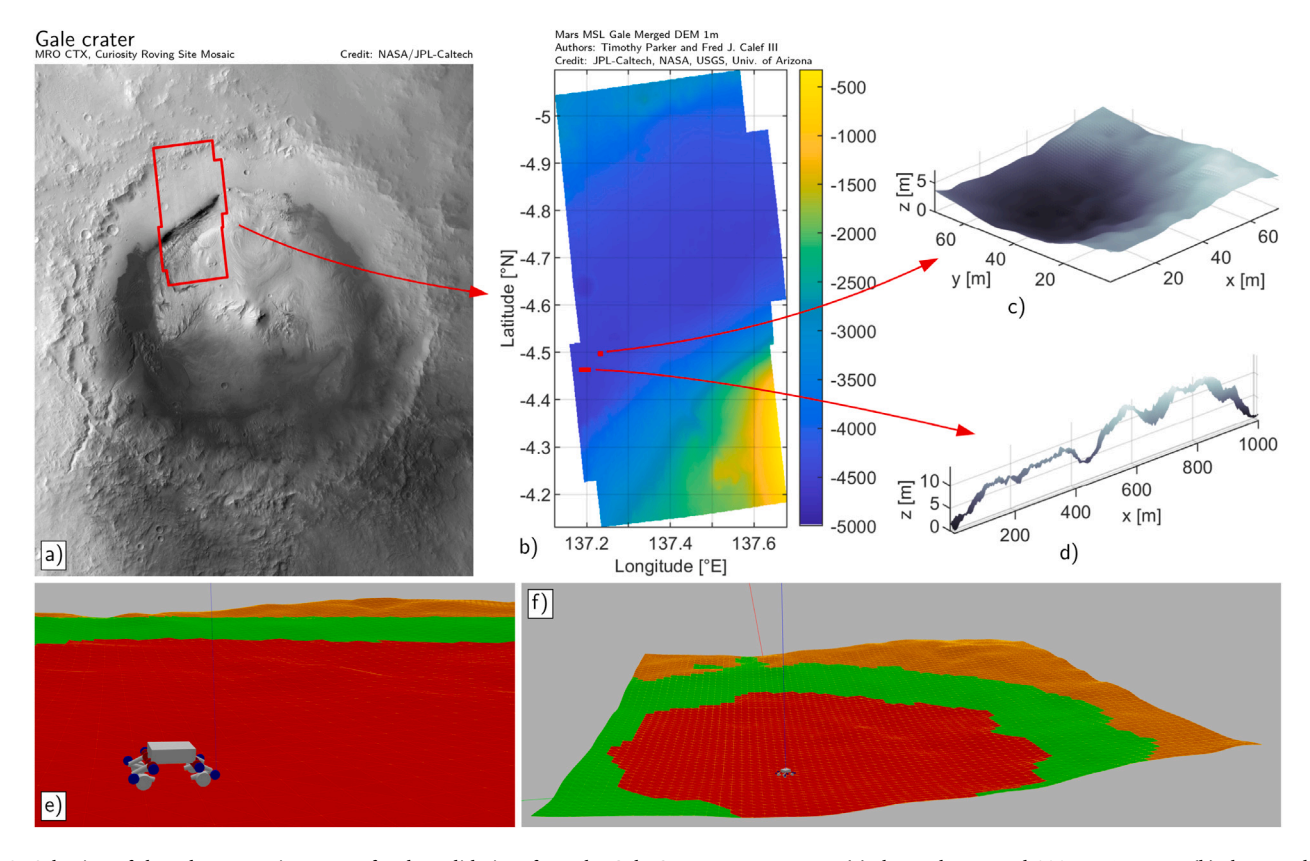


Fig. 6. Selection of the relevant environments for the validation, from the Gale Crater area, on Mars. (a) shows the general 300×400 km area; (b) shows a digital elevation map based on HiRISE data; (c) the crater environment; (d) the long-range drive environment; (e) the implementation of the TRP in Gazebo; (f) a snapshot of the crater environment which shows the three terrains defined in Table 5.

The wheels driving velocities and steering angles are then computed by a second controller module, based on the ICR projection approach described in [18,50].

As mentioned before, the hip and knee joints of the TRP rover can also be actuated, e.g. for the manipulation and positioning of the PMs or for compensation of the body orientation. These features, though, are beyond the scope of the following simulations. As such, the hip and knee joints actuators are kept passive in these simulations, while their positions are selected from the "XOAM" stances (Table 1) at the beginning of each run and are not changed afterwards.

## 4.3. Dataset specifications

A dataset is built with the results, by marking whether the run is uphill or downhill (in the crater environment), with or without a 20 kg payload, the selected "XOAM" stance and whether the kinematics is parallel or serial (see Section 2.5.2). An overview on the main parameters of the study is shown in Table 6. For each run, several parameters were saved during the simulation; a comprehensive list is given in Table 6. Regarding the stability evaluation, the maximum toppling moments acting on the rover have been calculated according to the stability polytope analysis described in [51]. The stability index is then obtained by normalizing the toppling moments and rearranging them such that 0-values indicate the most stable conditions, while 1-values are associated with the least stable ones.

When computing aggregate data for each run, we elected to use the 0.95 quantile level throughout the dataset. This choice stems from the fact that we are more interested in the prevalence of extreme values rather than averages, e.g. hip torques, ground clearance. However, maximum/minimum values are a poor indicator when numerical noise and spikes are frequent, as in this case.

**Table 6**Validation parameters and performance metrics. The range for each metric is given by considering the expected values within the scope of the simulations.

Parameters	Possible states	
Leg kinematics configuration	[serial, parallel]	
Stance	[X, O, A, M]	
Payload state	[true, false]	
Uphill (crater environment)	[true, false]	
Performance metrics	Expected range	
Stability	0-1	
Ground clearance	0.15-0.45 m	
Power consumption	0-2500 W	
Slip	0-1	
Hip torque	0-100 N m	
Knee torque	0-50 N m	

In the following, we present simplified implementations of the scenarios defined in the previous section: *long-range motion*, relevant for sensor networks, transport of modules for base-building, and *material transport*, relevant for mining, ISRU operations and sample collection.

At the end of this section, we discuss the results in a cohesive way, in order to gain insight on the implementation presented in this work, which revolves around the TRP rover.

## 4.4. Long-range motion: base building and sensor network

This set of simulations represents the long-distance travel instances in the *sensor network* scenario, described in Section 3.1; the CR is used to carry PMs at high speed over harsh but roughly level terrain, for long stretches. The dataset consists of 20 different paths generated by adding random noise to a general 1 km long straight path, each one traveled by the 16 possible combinations of legs kinematics configuration, stance

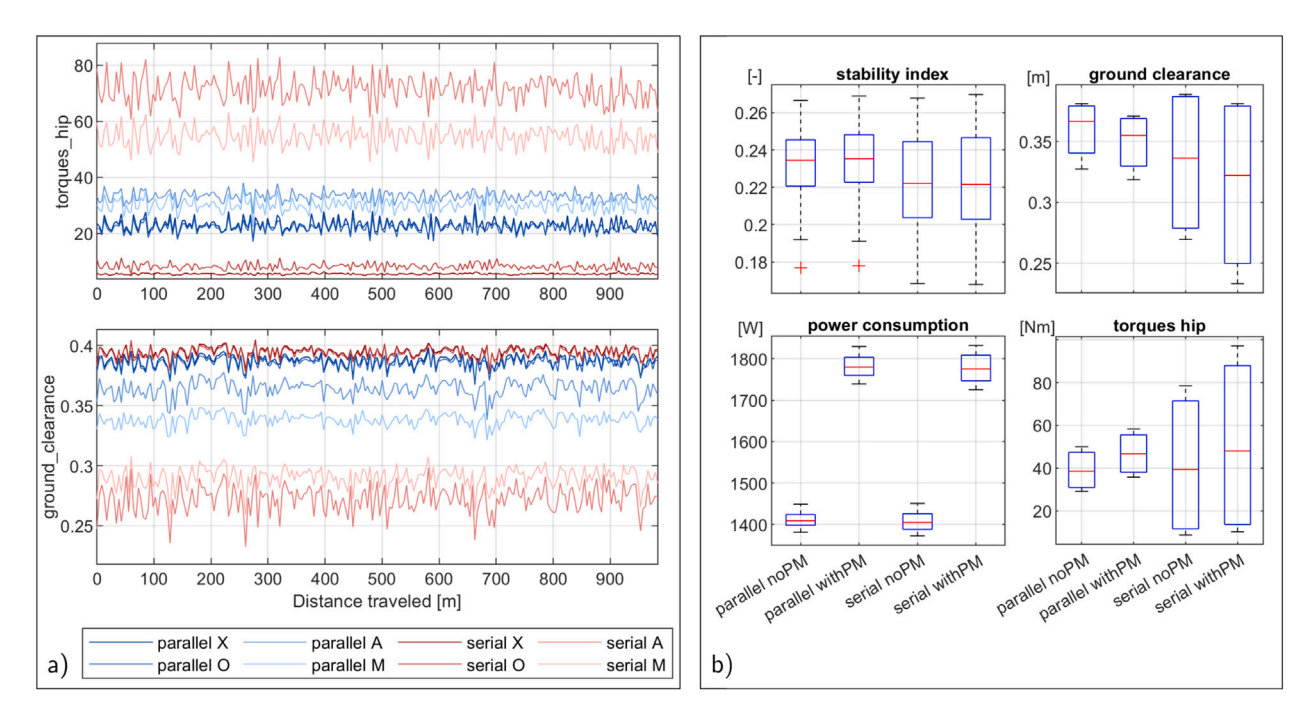


Fig. 7. Results of *long-range motion* scenario simulations, grouped by legs kinematics. (a) Time-domain evolution of ground clearance and hip torques across the full configuration set. (b) Aggregate results for a broader set of parameters, grouped by payload state – all "XOAM" stances are included in equal parts.

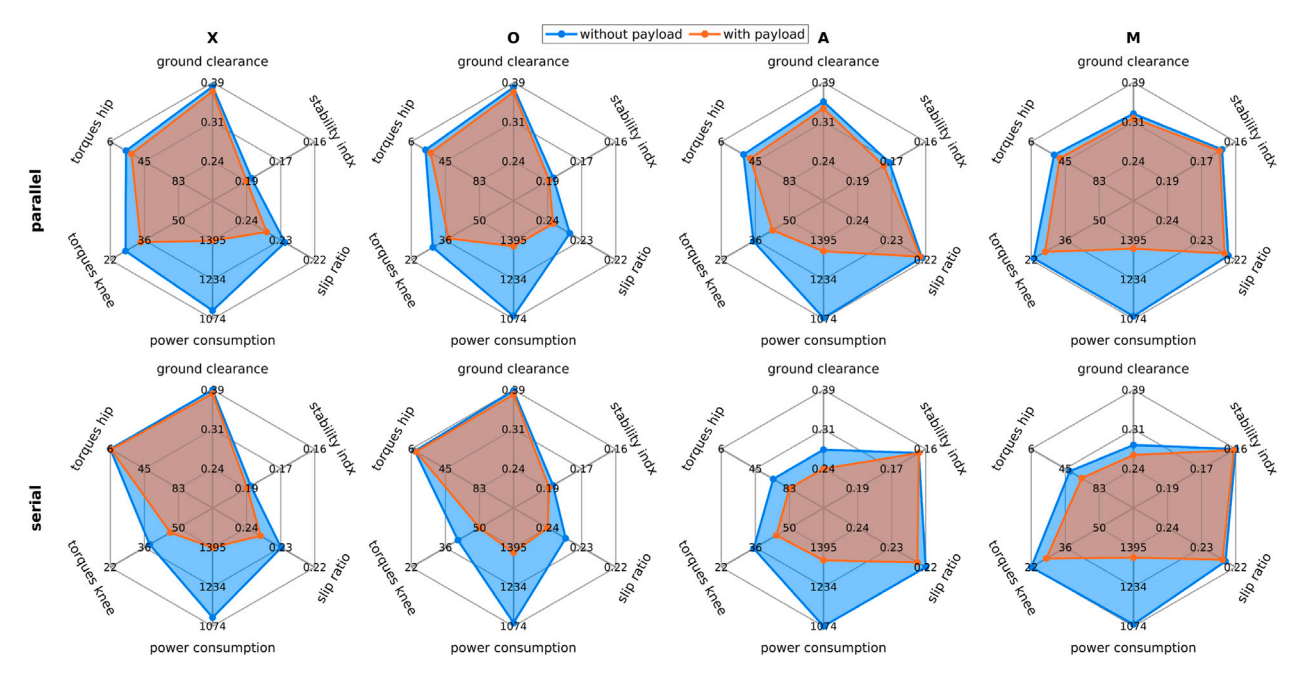


Fig. 8. Star plots showing the performance across the configuration set, depending on the presence of the payload and the kinematics of the legs. The dataset includes all runs from the "Crater" (limited to uphill), and from the "long-range" environments.

and payload state (Table 6), for a total of 320 runs. In this case, the CR travels both with and without payload; this impacts most parameters. Power consumption is strongly affected, as visible in Fig. 10b and c, and in Fig. 7b, showing values roughly 25 % higher.

The boxplots in Fig. 7b show data aggregated by serial/parallel kinematics and PM state. Stances ("XOAM") are distributed evenly in the simulations. The rationale for this is that, since the robot may change its stance midway, this representation gives insight on the *overall* capability of serial vs. parallel kinematics. Torques in the hip show very large variations in the case of *serial* kinematics stances; similarly this is visible for ground clearance. From the same figure,

it appears that the stability index is not especially affected by the kinematics, with a small advantage to *serial* configurations.

## 4.5. Material transport: water ice extraction

In this scenario, we focus on the *extraction phase* described in Section 3.2; the CR is used to ferry material (e.g. water ice) from the bottom of a crater up to an unloading area. After each traverse, the rover goes back to the base of the crater to gather more material. In order to simulate this in the most general way, we set up a set of five different preferred pathways across the rim of the crater (Fig. 10d),

S. Seriani et al. Acta Astronautica 238 (2026) 1189–1204

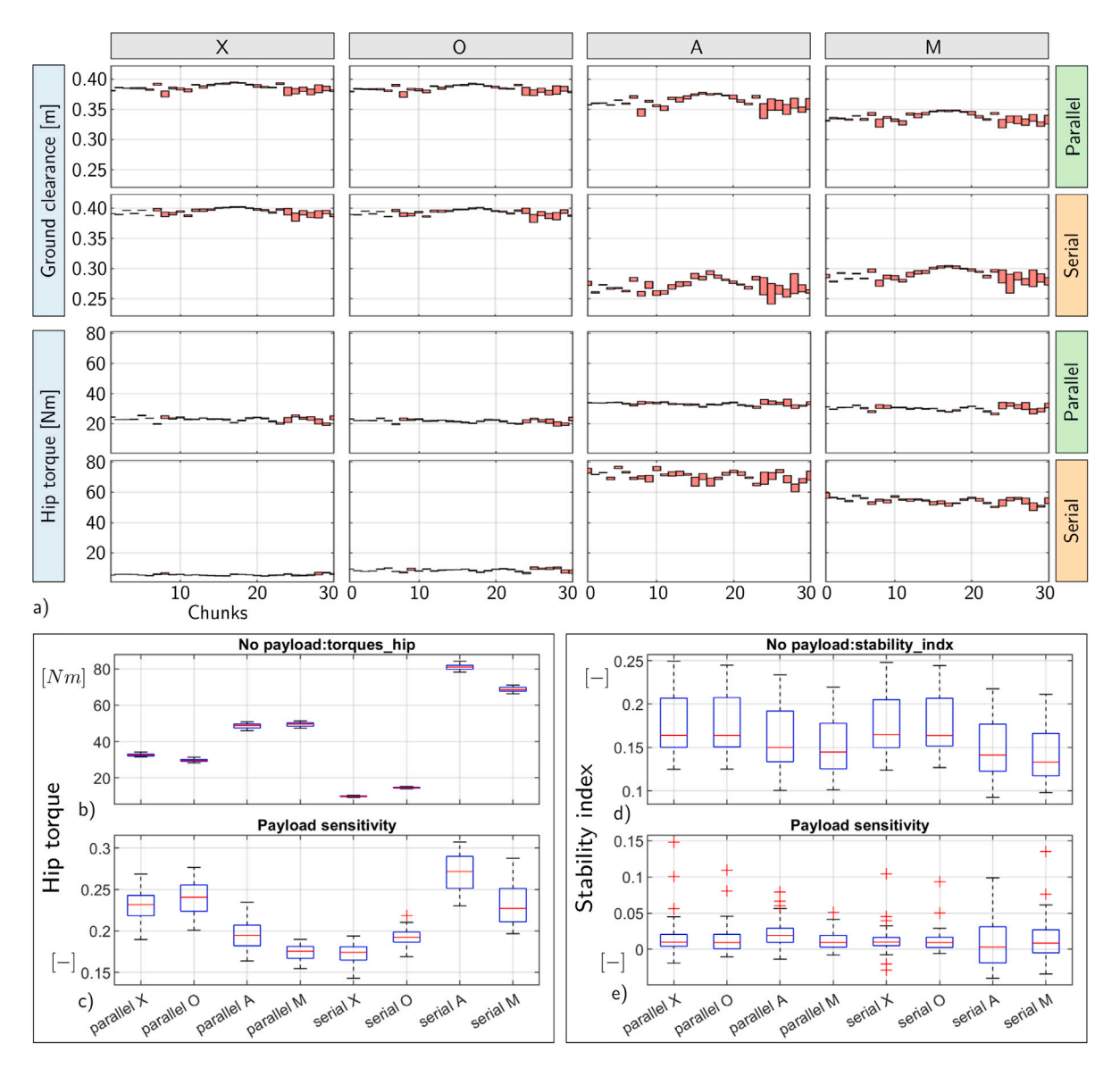
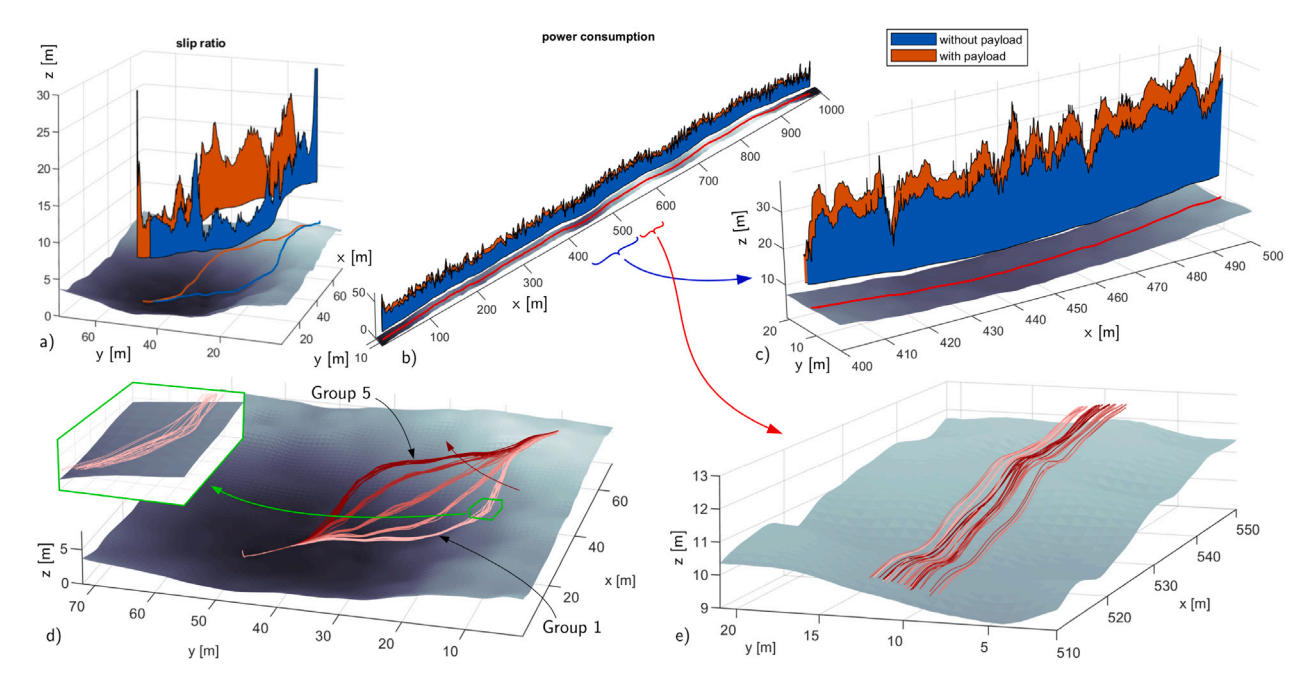


Fig. 9. Simulation results of the water-ice extraction scenario. (a) Time-domain analysis of a single group of trajectories. The evolution of ground clearance and hip torques are shown across the full configuration set. Data is aggregated in chunks based on traveled distance from the start, for comparison of different runs. (b–e) Results of the water-ice extraction simulation; distribution of the 0.95 quantile of each individual run. (b) hip torques across the configuration set; (c) sensitivity to the added payload of the hip torque across the configuration set; (d) stability index across the configuration set; (e) sensitivity to the added payload of the stability index across the configuration set.

while keeping the same end-points. For each of these, we generate ten proper paths by adding random noise to each waypoint. An example of these runs is shown in Fig. 10a, where an uphill and a downhill trajectories are illustrated along with the measured slip ratio. Results show that the configuration of the legs (both the stance and kinematics) do in fact influence many of the explored parameters. In particular, the evolution of the ground clearance varies considerably depending on the kinematics and stance of the legs, as visible in Fig. 9. For the ground clearance time-domain results clearly show that parallel and serial "X" and "O" configurations are unaffected, configurations "A" and "M" show degraded performance, especially with serial kinematics. The hip torque, on the other hand shows a more complex behavior, as confirmed by the statistical analysis in the same Figure (letters b-\*e): stances "A" and "M" show both the highest values of torque (serial) and lowest (parallel), while "X" and "O" show intermediate values in both kinematics configurations. Stances "X" and "O" seem the best candidates for torque value itself, but show high sensitivity to the payload compared to other configurations and stances.

#### 4.6. Discussion

The vast amount of data gathered in the simulations allows us to investigate the general space of the configurations of the TRP rover; in particular, two aspects were used as grouping factors in the analyses: the kinematic configuration of the legs, i.e. whether serial or parallel (see Fig. 3b and c), and the stance, i.e. the "XOAM" arrangement of the legs (see Fig. 4). The parameters that were considered as performance metrics (Table 6) reflect a diverse set of capabilities of the TRP that may be desirable to negotiate the tasks that are part of the mission. Therefore, it is not the intent of this work to identify a "best" configuration, but rather to give insight into how performance varies in the specific aspects, depending on the overall configuration of the rover given by the kinematic configuration, and stance. By looking at the "spider plots" in Fig. 8, we can see that performance across the configuration set varies depending on the presence of the payload, as one would expect. However, there is substantial difference on the magnitude of the change depending on the serial/parallel kinematics and "XOAM"



**Fig. 10.** Implementation of the environments and illustration of a Time-domain analysis on the crater and long-range environments. (a) slip ratio profile downhill (blue) without payload, uphill (red) with 20 kg payload; (b) power draw profile in long-range motion simulations with and without payload; (c) detail of (b) in the 400–500 m range; (d) structure of the paths in the crater for the simulations; (e) detail of the paths for the long-range motion scenario.

stance. In particular, serial-A configuration shows large performance decrease in all parameters with the exception of stability index and slip ratio, which, however, have very low sensitivity to payload state in all cases. Notably, a large increase in torque in the hip and a decrease in ground clearance are visible.

In the effort of producing meaningful data for evaluating performance across the configuration set, we elected to present scores for the parameters as shown in Table 7. First of all, for each of the six parameters, the variability is shown, which conveys the relevance of the parameter itself. It is immediately apparent that the most relevant is hip torque, followed by knee torque and ground clearance. The other parameters seem not to be affected substantially by the configuration of the rover legs. By considering these relevant parameters only, the overall score is 21 stars for the parallel kinematics against 17 for the serial.

The bottom part of the table shows the *insensitivity* to added payload, which translates into how much each parameter performance is worsened by the added mass of the PM. Between these, the only relevant parameters are the hip and knee torques. This is due to the fact that their variability is non-negligible both for their absolute value and their insensitivity to added payload (as a counter example, stability has a high variability value of 67.9%, but only 7.5% in its absolute value variability). The best performers seems the serial-X and parallel-M configurations.

In general, the main takeaways are the following:

- the parallel kinematics architecture shows reduced and less variable values in torque at the hip-joint (see Fig. 9a and b);
- the "X" and "O" stances show the lowest hip-joint torque values, especially in the serial kinematics architecture (see Fig. 9a and b).
- the parallel kinematics architecture shows larger and more stable values in ground clearance (see Fig. 9, and especially Fig. 7b);
- the "A" and "M" stances shows unacceptably low ground clearance in the serial kinematics architecture (see Table 7, and especially Fig. 7b);

- the stability index seems to be largely unaffected by the legs configuration, with slightly better values for "A" and "M" configurations in both serial and parallel kinematics architectures (see Fig. 9d and Table 7)
- power consumption seems to be affected only by the added mass of the payload (see Fig. 7b), and in the same way in all configurations (see its low absolute-value variability in Table 7);

As a final remark, the tests presented here indicate pretty clearly that there is no such thing as an *overall* best configuration, neither in terms of kinematics structure (parallel or serial), nor in terms of stance ("X", "O", "A" or "M"). Most of the configurations have strengths and weaknesses, with possibly the exception of serial-A and M, which show a tendency to yielding under the rover's own weight more than what could be considered safe.

#### 5. Conclusion

In this work we have presented a vision for space exploration that revolves around a modular architecture consisting of two main agents: a carrier rover and a set of payload modules. We have illustrated the core principles and the main characteristics of the infrastructure: a classification of modules (standalone/non-standalone), the requirements and capabilities of the carrier rover. Significant space was given to an overview of activities that are enabled by the proposed approach, from prime activities (power supply, communication relay etc.) to higher-level activities such as networks (e.g. geophysical sensor arrays) and assemblies (e.g. precursor bases, ISRU). Considerable insight was given for the development of the carrier rover, including its kinematics architecture (serial/parallel knee actuation), its actuation scheme, and several general implementation details of its locomotion system. We have elected to define a fixed set of four stances identified with the letters "XOAM", in order to represent the parameter space of the legs geometrical configuration.

To provide justification for the proposed approach, we selected two complex scenarios: the deployment of a sensor network on Mars, and an ISRU activity. In the former, we provided both a qualitative

Table 7
Grouped comparison of the performance of serial and parallel kinematics across different stances in the case of the "water ice extraction" scenario. The analysis is score-based, with higher scores (more stars) showing better performance in the related area. The variability scores show the percentage of variation across each column normalized on the column's mean.

			Performance scores	<ul> <li>absolute values</li> </ul>			
		Stability	Clearance	Power Cons.	Slip	Hip torque	Knee torque
	$Variability \rightarrow$	7.5%	12.0%	1.5%	3.8%	30.7%	17.2%
Kinematics	Stance						
	X	☆	***	*	**	**	**
Parallel	0	☆	***	**	*	**	**
Parallel	A	*	**	***	**	*	☆
	M	**	*	**	***	*	**
	X	☆	***	☆	**	***	☆
01-1	0	☆	***	**	☆	***	☆
Serial	A	***	\$	***	***	☆	**
	M	***	☆	**	*	☆	***
		Perf	ormance scores – inser	sitivity to added payload			
		Stability	Clearance	Power Cons.	Slip	Hip torque	Knee torque
	$Variability \rightarrow$	67.9%	29.5%	2.0%	51.4%	13.0%	10.5%
Kinematics	Stance						
	X	**	***	*	*	*	**
Parallel	0	**	***	☆	*	*	**
Parallel	A	☆	**	***	***	**	***
	M	**	***	**	***	***	***
	X	**	***	**	☆	***	***
0 : 1	0	**	***	☆	*	**	***
Serial	A	***	<b>*</b>	***	**	☆	☆
	M	**	**	***	***	*	☆

analysis of our vision against two state-of-the-art approaches (separate landers, and sensorized rovers); based on past missions, we proposed a preliminary quantitative analysis of the entry stage mass, against the same existing approaches, showing that our vision has merit when the number of deployed sensors is larger than 3–6, depending on many factors. In the latter, we break down a prototypical ISRU activity like water ice extraction, built specifically around the carrier rover and payload module architecture we propose in this work.

The scenarios acted as the backdrop for the validation of our proposed architecture, where we showed in detail a simulated implementation of the carrier rover traveling over diverse terrains in the region of the Gale crater, on Mars. The comprehensive set of more than 1500 simulation runs was designed to capture different moments of the scenarios, e.g. the transport of material from the bottom of a crater and the return trip while empty. We show in particular how the behavior of the carrier rover changes depending on the added mass from the payload module (sensor network scenario) and from transported material (ISRU activity). Results show the performance metrics variations depending on the selected kinematics (i.e. serial/parallel) and stance (i.e. "XOAM"), highlighting the fact that there is no clear winner. Nevertheless, statistical analysis enabled us to isolate several takeaway points, which we discussed in detail.

Building on these developments, we plan on extending and deepening our current vision for robotic space exploration and settlement; in particular, we foresee the following activities as part of our future research in this field:

- An in-depth parameter space exploration of the stance (leg's hip/ knee angles, ground clearance, wheelbase) and its influence on the main performance metrics;
- Development of strategies for active stance control, especially during fast driving scenarios;
- Implementation of a framework to enable the *simulation of assembly* using the carrier rover and payload module infrastructure;

Part of these activities are already in active development, and in the future may contribute to the backbone of a new, more autonomous and more capable generation of agents for exploring our neighbors in the Solar System.

### CRediT authorship contribution statement

S. Seriani: Supervision, Methodology, Conceptualization. M. Caruso: Software, Methodology. S. Cottiga: Validation, Software. P. Gallina: Writing – review & editing, Writing – original draft. M. Görner: Writing – review & editing, Supervision. A. Wedler: Writing – review & editing, Supervision.

#### **Funding**

This work was partially funded by: the European Union - Next Generation EU, Mission 4 Component 1, CUP J53D23007120001, project AI4FOREST; the "Fondo Ricerca di Ateneo" FRA 2025, of the Department of Engineering and Architecture, University of Trieste.

### Declaration of competing interest

The authors declare that they have no known competing financial interests or personal relationships that could have appeared to influence the work reported in this paper.

#### References

- S. Cottiga, M. Caruso, P. Gallina, S. Seriani, Proprioceptive swarms for celestial body exploration, Acta Astronaut. 223 (2024) 159–174, cited By 1.
- [2] Y. Zou, Y. Zhu, Y. Bai, L. Wang, Y. Jia, W. Shen, Y. Fan, Y. Liu, C. Wang, A. Zhang, G. Yu, J. Dong, R. Shu, Z. He, T. Zhang, A. Du, M. Fan, J. Yang, B. Zhou, Y. Wang, Y. Peng, Scientific objectives and payloads of Tianwen-1, China's first Mars exploration mission, Adv. Space Res. 67 (2) (2021) 812–823, Cited by: 192; All Open Access, Hybrid Gold Open Access.
- [3] J.E. Graf, R.W. Zurek, H.J. Eisen, B. Jai, M. Johnston, R. Depaula, The mars reconnaissance orbiter mission, Acta Astronaut. 57 (2–8) (2005) 566–578, Cited by: 68.
- [4] T.L. Huntsberger, A. Trebi-Ollennu, H. Aghazarian, P.S. Schenker, P. Pirjanian, H.D. Nayar, Distributed control of multi-robot systems engaged in tightly coupled tasks, Auton. Robots 17 (1) (2004) 79–92, Cited by: 67.
- [5] B. Foing, From SMART1 and recent probes towards artemis and a human/robotic moon village, 2877, (1) 2024, Cited by: 0; All Open Access, Gold Open Access.
- [6] M.E. Evans, L.D. Graham, A flexible lunar architecture for exploration (FLARE) supporting nasa's artemis program, Acta Astronaut. 177 (2020) 351–372, Cited by: 50; All Open Access, Green Open Access.

- [7] R.A. Lindemann, D.B. Bickler, B.D. Harrington, G.M. Ortiz, C.J. Voorhees, Mars exploration rover mobility development - mechanical mobility hardware design, development, and testing, IEEE Robot. Autom. Mag. 13 (2) (2006) 19–26, Cited by: 105.
- [8] L. Burkhard, R. Sakagami, K. Lakatos, H. Gmeiner, P. Lehner, J. Reill, M.G. Müller, M. Durner, A. Wedler, Collaborative multi-rover crater exploration: Concept and results from the ARCHES analog mission, 2024, Cited by: 1; All Open Access, Green Open Access.
- [9] S. Seriani, P. Gallina, A. Wedler, Dynamics of a tethered rover on rough terrain, Mech. Mach. Sci. 47 (2017) 355–361, cited By 11.
- [10] E. Staudinger, R. Giubilato, M.J. Schuster, R. Pöhlmann, S. Zhang, A. Dömel, A. Wedler, A. Dammann, Terrain-aware communication coverage prediction for cooperative networked robots in unstructured environments, Acta Astronaut. 202 (2023) 799–805, Cited by: 4; All Open Access, Green Open Access.
- [11] J. Bob Balaram, T. Canham, C. Duncan, M. Golombek, H.a.F.r. Grip, W. Johnson, J. Maki, A. Quon, R. Stern, D. Zhu, Mars helicopter technology demonstrator, 2018, Cited by: 183.
- [12] T. Tzanetos, M. Aung, J. Balaram, H.F. Grip, J.T. Karras, T.K. Canham, G. Kubiak, J. Anderson, G. Merewether, M. Starch, M. Pauken, S. Cappucci, M. Chase, M. Golombek, O. Toupet, M.C. Smart, S. Dawson, E.B. Ramirez, J. Lam, R. Stern, N. Chahat, J. Ravich, R. Hogg, B. Pipenberg, M. Keennon, K.H. Williford, Ingenuity mars helicopter: From technology demonstration to extraterrestrial scout, 2022-March, 2022, Cited by: 39.
- [13] Y. Zou, Y. Zhu, Y. Bai, L. Wang, Y. Jia, W. Shen, Y. Fan, Y. Liu, C. Wang, A. Zhang, G. Yu, J. Dong, R. Shu, Z. He, T. Zhang, A. Du, M. Fan, J. Yang, B. Zhou, Y. Wang, Y. Peng, Scientific objectives and payloads of tianwen-1, China's first mars exploration mission, Adv. Space Res. 67 (2) (2021) 812–823, Cited by: 86; All Open Access, Hybrid Gold Open Access.
- [14] A. Rankin, M. Maimone, J. Biesiadecki, N. Patel, D. Levine, O. Toupet, Mars curiosity rover mobility trends during the first 7 years, J. Field Robot. 38 (5) (2021) 759–800, Cited by: 31.
- [15] K.A. Farley, K.H. Williford, K.M. Stack, R. Bhartia, A. Chen, M. de la Torre, K. Hand, Y. Goreva, C.D.K. Herd, R. Hueso, Y. Liu, J.N. Maki, G. Martinez, R.C. Moeller, A. Nelessen, C.E. Newman, D. Nunes, A. Ponce, N. Spanovich, P.A. Willis, L.W. Beegle, J.F. Bell, A.J. Brown, S.-E. Hamran, J.A. Hurowitz, S. Maurice, D.A. Paige, J.A. Rodriguez-Manfredi, M. Schulte, R.C. Wiens, Mars 2020 mission overview, Space Sci. Rev. 216 (8) (2020) Cited by: 385.
- [16] D. Rodríguez-Martínez, M. Van Winnendael, K. Yoshida, High-speed mobility on planetary surfaces: A technical review, J. Field Robot. 36 (8) (2019) 1436–1455, Cited by: 29.
- [17] M. Caruso, L. Bregant, P. Gallina, S. Seriani, Design and multi-body dynamic analysis of the archimede space exploration rover, Acta Astronaut. 194 (2022) 229–241. cited By 14.
- [18] M. Caruso, M. Giberna, M. Görner, P. Gallina, S. Seriani, The archimede rover: A comparison between simulations and experiments, Robotics 12 (5) (2023) cited By 2.
- [19] F. Abilleira, 2011 mars science laboratory launch period design, 142, 2012, pp. 2345–2364, Cited by: 1.
- [20] F. Poulet, C. Gross, B. Horgan, D. Loizeau, J.L. Bishop, J. Carter, C. Orgel, Mawrth vallis, mars: A fascinating place for future in situ exploration, Astrobiology 20 (2) (2020) 199–234, Cited by: 21; All Open Access, Green Open Access
- [21] I.E. Jehn, C.B. Dreyer, A design methodology for flat slab lunar landing and launch pad systems, Acta Astronaut. 231 (2025) 175–192, Cited by: 0; All Open Access, Hybrid Gold Open Access.
- [22] S. Boazman, D. Heather, E. Sefton-Nash, C. Orgel, B. Houdou, X. Lefort, Scientific analysis and accessibility of potential landing sites for esa's PROSPECT instrument, 2022-September, 2022, Cited by: 0.
- [23] M. De Benedetti, S. Kay, J. Ocon, R. Jalvo, M.E. Cerezo, A. Gomez Eguiluz, M. Alonso, J.R. Fernandez, K. Buckley, R. Field, A. Cameron, V. Papantoniou, A. Papantoniou, C.P. Del Pulgar, K. Kapellos, M. Azkarate, RAPID & FASTNAV projects: High-speed semi-autonomous rovers enabling high return planetary missions, in: 2024 International Conference on Space Robotics, ISpaRo 2024, 2024, pp. 260–265, Cited by: 0.
- [24] F. Cordes, F. Kirchner, A. Babu, Design and field testing of a rover with an actively articulated suspension system in a mars analog terrain, J. Field Robot. 35 (7) (2018) 1149–1181, Cited by: 72; All Open Access, Green Open Access.
- [25] B. Zhu, J. He, J. Sun, Kinematic modeling and hybrid motion planning for wheeled-legged rovers to traverse challenging terrains, Robotica 42 (1) (2024) 153–178, Cited by: 3.
- [26] V.S. Medeiros, E. Jelavic, M. Bjelonic, R. Siegwart, M.A. Meggiolaro, M. Hutter, Trajectory optimization for wheeled-legged quadrupedal robots driving in challenging terrain, IEEE Robot. Autom. Lett. 5 (3) (2020) 4172–4179, Cited by: 71; All Open Access. Green Open Access.
- [27] A.F. Prince, B. Vodermayer, B. Pleintinger, A. Kolb, G. Franchini, E. Staudinger, E. Dietz, S. Schröder, S. Frohmann, F. Seel, A. Wedler, Modular mechatronics infrastructure for robotic planetary exploration assets in a field operation scenario. Acta Astronaut. 212 (2023) 160–176.
- [28] S. Seriani, P. Gallina, L. Scalera, A. Gasparetto, A. Wedler, A new mechanism for the deployment of modular solar arrays: Kinematic and static analysis, 2018, pp. 372–379, cited By 1.

- [29] M.T. Thorpe, T.F. Bristow, E.B. Rampe, N.J. Tosca, J. Grotzinger, K. Bennett, C. Achilles, D. Blake, S. Chipera, G. Downs, R. Downs, S. Morrison, V. Tu, N. Castle, P. Craig, D.J.D. Marais, R. Hazen, D. Ming, R. Morris, A. Treiman, D. Vaniman, A. Yen, A. Vasavada, E. Dehouck, J. Bridges, J. Berger, A. McAdam, T. Peretyazhko, K. Siebach, A. Bryk, V. Fox, C. Fedo, Mars science laboratory CheMin data from the Glen Torridon Region and the significance of lake-groundwater interactions in interpreting mineralogy and sedimentary history, J. Geophys. Res.: Planets 127 (11) (2022) Cited by: 57; All Open Access, Green Open Access, Hybrid Gold Open Access.
- [30] P. Lehner, S. Brunner, A. Dömel, H. Gmeiner, S. Riedel, B. Vodermayer, A. Wedler, Mobile manipulation for planetary exploration, 2018-March, 2018, pp. 1–11, http://dx.doi.org/10.1109/AERO.2018.8396726, Cited by: 30; All Open Access, Green Open Access, URL https://www.scopus.com/inward/record.uri?eid=2-s2.0-85049867678&doi=10.1109%2fAERO.2018.8396726&partnerID=40&md5=dc863fefa059ed342982f80a1ac30e49.
- [31] C. Yana, R. Lapeyre, E. Gaudin, K. Hurst, P. Lognonné, L. Rochas, Deployment and surface operations of the SEIS instrument onboard the InSight mission, Acta Astronaut. 202 (2023) 772–781, Cited by: 3; All Open Access, Bronze Open Access.
- [32] P. Zhang, W. Dai, R. Niu, G. Zhang, G. Liu, X. Liu, Z. Bo, Z. Wang, H. Zheng, C. Liu, H. Yang, Y. Bai, Y. Zhang, D. Yan, K. Zhou, M. Gao, Overview of the lunar in situ resource utilization techniques for future lunar missions, Space: Sci. Technol. (United States) 3 (2023) Cited by: 43; All Open Access, Gold Open Access.
- [33] Y. Ou, H. Zhang, W. Zheng, Y. Wang, Autonomous land beacon selection for spacecraft navigation around mars, 2017-January, 2017, pp. 2707–2710, Cited by: 2.
- [34] Y. Ou, H. Zhang, Mars final approach navigation using ground beacons and orbiters: An information propagation perspective, Acta Astronaut. 138 (2017) 490–500, Cited by: 11.
- [35] A.-M. Harri, K. Pichkadze, L. Zeleny, L. Vazquez, W. Schmidt, S. Alexashkin, O. Korablev, H. Guerrero, J. Heilimo, M. Uspensky, V. Finchenko, V. Linkin, I. Arruego, M. Genzer, A. Lipatov, J. Polkko, M. Paton, H. Savijärvi, H. Haukka, T. Siili, V. Khovanskov, B. Ostesko, A. Poroshin, M. Dlaz-Michelena, T. Siikonen, M. Palin, V. Vorontsov, A. Polyakov, F. Valero, O. Kemppinen, J. Leinonen, P. Romero, The MetNet vehicle: A lander to deploy environmental stations for local and global investigations of Mars, Geosci. Instrum. Methods Data Syst. 6 (1) (2017) 103–124, Cited by: 10; All Open Access, Gold Open Access, Green Open Access.
- [36] G. Pont, P. Lognonné, S. de Raucourt, T. Kawamura, T. Nebut, O. Robert, S. Tillier, G. Chabaud, R. Garcia, M. Panning, E. Miller, F. IJpelaan, Lunar seismometers: Past, present and future, 1A, 2024, pp. 205–213, Cited by: 0.
- [37] J. Olsen, Impacts of low-power requirements on the LEMS HMS design, IEEE Women Eng. Mag. 17 (1) (2023) 32–37, Cited by: 0.
- [38] R. Capozzi, M. Wilde, B. Kish, Daisy chain navigation and communication in underground environments, 2021-March, 2021, Cited by: 2.
- [39] B. Mukanova, Control of actuators torques for optimal movement along a given trajectory for the dextar robot, J. Appl. Comput. Mech. 7 (1) (2021) 165–176, Cited by: 3.
- [40] D.W. Way, R.W. Powell, A. Chen, A.D. Steltzner, A.M.S. Martin, P.D. Burkhart, G.F. Mendeck, Mars science laboratory: Entry, descent, and landing system performance, 2007, Cited by: 95; All Open Access, Green Open Access.
- [41] P.N. Desai, J.L. Prince, E.M. Queen, M. Schoenenberger, J.R. Cruz, M.R. Grover, Entry, descent, and landing performance of the mars phoenix lander, J. Spacecr. Rockets 48 (5) (2011) 798–808, Cited by: 97; All Open Access, Green Open Access
- [42] B. Gopalchetty, Martian hydrosphere: A brief overview of water on mars, New Astron. Rev. 100 (2025) Cited by: 1.
- [43] P.O. Hayne, A. Hendrix, E. Sefton-Nash, M.A. Siegler, P.G. Lucey, K.D. Retherford, J.-P. Williams, B.T. Greenhagen, D.A. Paige, Evidence for exposed water ice in the moon's south polar regions from lunar reconnaissance orbiter ultraviolet albedo and temperature measurements, Icarus 255 (2015) 58–69, Cited by: 258.
- [44] C. Schwandt, J.A. Hamilton, D.J. Fray, I.A. Crawford, The production of oxygen and metal from lunar regolith, Planet. Space Sci. 74 (1) (2012) 49–56, Cited by: 145
- [45] K. Zacny, P. Chu, G. Paulsen, A. Avanesyan, J. Craft, L. Osborne, Mobile insitu water extractor (MISWE) for mars, moon, and asteroids in situ resource utilization, 2012, Cited by: 56.
- [46] N. Koenig, A. Howard, Design and use paradigms for gazebo, an open-source multi-robot simulator, in: 2004 IEEE/RSJ International Conference on Intelligent Robots and Systems (IROS) (IEEE Cat. No.04CH37566), vol. 3, 2004, pp. 2149–2154 vol.3, http://dx.doi.org/10.1109/IROS.2004.1389727.
- [47] C. Pavlov, A.M. Johnson, A terramechanics model for high slip angle and skid with prediction of wheel-soil interaction geometry, J. Terramechanics 111 (2024) 9–19, Cited by: 4.

- [48] R. Zhou, W. Feng, L. Ding, H. Yang, H. Gao, G. Liu, Z. Deng, MarsSim: A high-fidelity physical and visual simulation for mars rovers, IEEE Trans. Aerosp. Electron. Syst. 59 (2) (2023) 1879–1892, Cited by: 19.
- [49] L. Ding, Z. Deng, H. Gao, J. Tao, K.D. Iagnemma, G. Liu, Interaction mechanics model for rigid driving wheels of planetary rovers moving on sandy terrain with consideration of multiple physical effects, J. Field Robot. 32 (6) (2015) 827–859, Cited by: 91; All Open Access, Bronze Open Access.
- [50] M. Caruso, N. Sesto Gorella, P. Gallina, S. Seriani, Towing an object with a rover, J. Mech. Robot. 17 (2) (2024) 021001.
- [51] S. Seriani, P. Gallina, A. Wedler, A modular cable robot for inspection and light manipulation on celestial bodies, Acta Astronaut. 123 (2016) 145–153, cited By 37.